

The Effect of the Soft Segment of Polyurethane on Copolymer-Type Polyacetal / Polyurethane Blends

WEN-YEN CHIANG and CHI-YUAN HUANG, *Department of Chemical Engineering, Tatung Institute of Technology, Taipei 10451, Taiwan, Republic of China*

Synopsis

Mechanical blends of copolymer-type polyacetal (POM) with ester-based and ether-based polyurethane (PU) are immiscible over the 0–50% PU compositional range. The PU elastomer was added to the rigid POM matrix to increase its toughness. The mechanical, physical, thermal, dielectric, and dynamic mechanical properties and morphology of POM/PU blends were investigated. The notched Izod-impact strength of blends reaches a maximum at 10 wt % PU. The tensile strength, Young's modulus, volume resistivity, crystallinity, and density decrease with increasing concentration of PU. The elongation of blends reaches a maximum at 20 wt % PU. The dielectric constant and dissipation factor increase with increasing PU content. From dynamic mechanical measurements, as the elastomer content increases, the height of the damping peak also increases, but there is no transition temperature shift. SEM shows that the blends exhibit a continuous morphology with domain size varying from 1 to 10 μm for PU. However, at a concentration of 50 wt % PU, the dispersed PU particles tend to aggregate. Characterization of morphology by a metallurgical microscope has shown that the crystalline materials in the pure POM and the blends exist in a spherulitic superstructure.

INTRODUCTION

Polyacetal (POM) resins are strong, hard, highly crystalline thermoplastics. They are engineering plastics with a unique balance of mechanical, thermal, chemical, and electrical properties. The resin has a good balance of both long- and short-term predictable properties. They exhibit substantial elongation in tensile tests and are highly fatigue resistant.¹

The toughness of many engineering thermoplastics can be improved by incorporation of a low modulus second component.² When highly dispersed, the rubbery phase acts as an effective stress concentrator³ and enhances both crazing and shear yielding in the matrix. Since both processes can absorb large amounts of energy, such materials typically exhibit superior resistance to crack propagation under impact conditions.

Like many unmodified polymer materials, they fail in a brittle manner when impacted, especially when stress risers are present.⁴ Product development has been concerned with improving in toughness and other properties of POM, especially in the use of elastomer-modified formulations, where toughness of POM is markedly increased. The elastomer-modified POM has been described in previous reports using polyurethane (PU).^{4–10} These works describe the use of melt blending to make toughened POM and reports on the properties of various compositions of the POM/PU system.

TABLE I
Description of the Composition of POM/PU Blends

Sample	POM ^a	PU ^b	POM/PU ^c
971	M90	CVP706AW	90/10
972	M90	CVP706AW	80/20
973	M90	CVP706AW	70/30
975	M90	CVP706AW	50/50
981	M90	S80A	90/10
982	M90	S80A	80/20
983	M90	S80A	70/30
985	M90	S80A	50/50
991	M90	S90A	90/10
992	M90	S90A	80/20
993	M90	S90A	70/30
995	M90	S90A	50/50
911	M90	1190A	90/10
912	M90	1190A	80/20
913	M90	1190A	70/30
915	M90	1190A	50/50

^aPolyacetal.

^bPolyurethane; CVP706AW: Shore A 70; S80A: Shore A 80; S90A and 1190A: Shore A 90.

^cWeight ratio.

EXPERIMENTAL

Materials

One commercial copolymer-type polyacetal, Duracon M90 (Japan Polyplas-tics Co. Ltd.) with melt flow index of 8, and four commercial polyurethanes, Elastollan 1190A (ether-based), CVP706AW, S80A, S90A (ester-based), all from Elastogran Polurethane-Elastomer GmbH, West Germany, were used. Table I is the description of the composition of M90/PU polyblends.

Melt Blending

The variety of compositions of POM/PU were compounded at weight ratios of 100/0, 90/10, 80/20, 70/30, and 50/50, and blended in an extruder. Test pieces were prepared by compression molding in a frame at 150 kg/cm² for 6 min, and then cooled by a water-cooling system. Dumbbell test pieces were made for mechanical testing.

Mechanical Properties

Tensile properties were measured according to the ASTM D638 test method using an Instron Universal Testing Machine Model 1130. The crosshead load was 500 kg, the speed was at 5 cm/min, and the chart speed was 100 cm/min. The elastic moduli were determined from the slope of the initial part of the stress-strain curve within the linear trend. The values obtained were averaged over many measurements. Notched Izod-impact strength was measured according to the ASTM D256 test method. The thickness was 0.3 ± 0.02 cm and the energy was 60 kg cm.

Thermal Properties

A DuPont Instrument 1090B Analyzer equipped with a 951 Thermogravimetric Analyzer (TGA) was used under nitrogen at a heating rate of 20°C/min to measure the thermal degradation of blends.

X-Ray Measurements

The wide-angle X-ray diffractograms (WAXD) were measured at room temperature on Rigaku D/MAX-III A X-ray diffractometer with FeK_α radiation generated at 40 kV and 20 mA. The scan rate used for the WAXD profiles was 1°/min. A teletype was connected to the terminal of the digital counter so that the counts were automatically recorded. The degree of crystallinity (X_c) was calculated from the diffraction peak by determining the ratio of the crystalline area to the total area.^{5,6}

Density Measurements

The density was measured at 23°C and was used to calculate the specific gravity of the plastics by displacement (ASTM D792). The calculation was described in previous papers.^{5,6}

Dielectric Properties

The volume resistivity of POM/PU blends were obtained at room temperature by using a volume resistivity tester of Type TR8601 from Takda Riken Co. The test voltage was 500 V and the charge time was 1 min. Dielectric constant (ϵ') and dissipation factor ($\tan \delta$) were tested by using a dielectric loss measuring unit of Type TR-10C (null detector: type BDA-9, oscillator: type WBG-9) according to ASTM D150.

Dynamic Mechanical Measurements

Dynamic mechanical data, loss tangent $\tan \delta$, and complex modulus E^* , were obtained with a Rheovibron dynamic viscoelastomer (Model DDV-II-C) at a heating rate 1–2°C/min and 110 Hz from –100 to 100°C. The correction due to clamp extension was applied at all temperatures.

SEM Photographs and Metallurgical Micrographs

For examination of phase morphology, compression-molded Izod bars were immersed in liquid nitrogen and fractured. These fracture surfaces were coated with gold and viewed end on by a Cambridge Stereoscan S4-10 scanning electron microscope. A compression-molded plastic of blends was examined under the metallurgical microscope.

RESULTS AND DISCUSSION

Mechanical Properties

In this investigation, the POM/PU blends have been prepared containing up to 50% by weight of polyurethane (PU). The stress-strain properties of

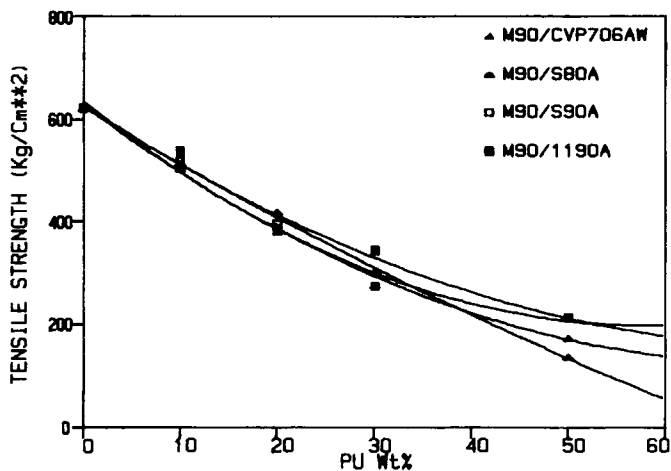


Fig. 1. Tensile strength of M90/PU blends: (Δ) M90/CVP706AW; (▲) M90/S80A; (□) M90/S90A; (■) M90/1190A.

POM/PU blends depend on composition, that is, tensile strength, Young's modulus, elongation, and impact strength vary with composition. Plots of tensile strength (Fig. 1) and modulus (Fig. 2) vs. blend composition both decrease with increasing PU content.

However, as seen in Figure 3, the percent elongation at break deviates markedly from additive values for pure POM and PU. It shows that the elongation of blends reaches a maximum at 20 wt % PU.

The rubbery PU was added to rigid POM matrix in order to increase the toughness and elongation of the POM breakpoint. It is known that tensile strength of toughened plastics decreases with rubber content, while elongation at breakpoint increases with a range of rubber content.¹¹

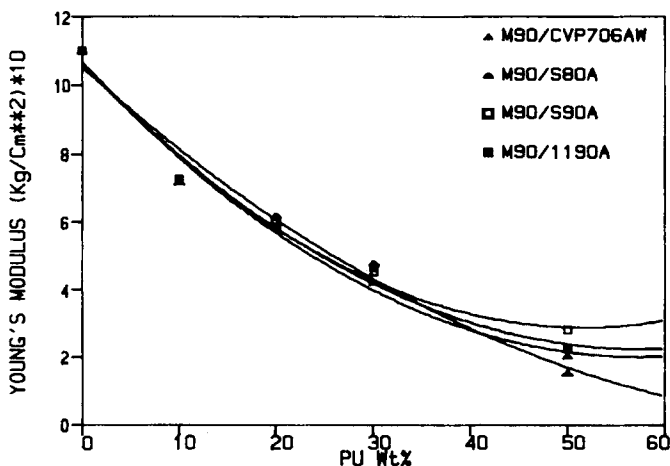


Fig. 2. Young's modulus of M90/PU blends: (Δ) M90/CVP706AW; (▲) M90/S80A; (□) M90/S90A; (■) M90/1190A.

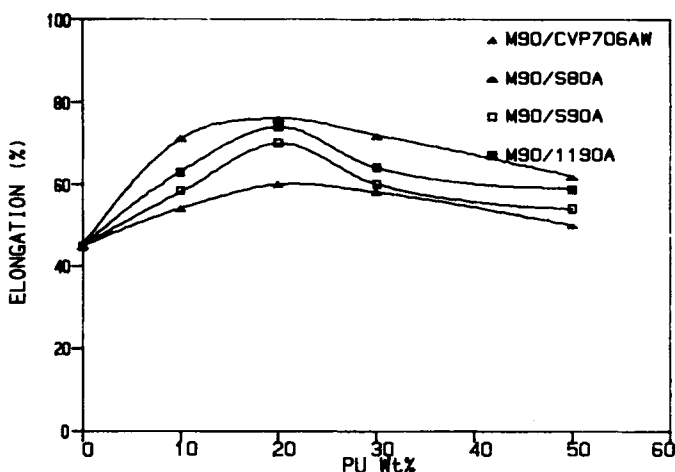


Fig. 3. Elongation of M90/PU blends: (△) M90/CVP706AW; (▲) M90/S80A; (□) M90/S90A; (■) M90/1190A.

Rubber Toughened

There are three principal ways of preparing blends with toughness or high impact resistance.¹² The original method involved blending by mechanical techniques. The second method is the solution-graft copolymer technique. The third method is emulsion polymerization. This study used the first method to prepare toughened plastic. The effectiveness of toughening with rubber depends on a number of factors including³:

- (a) the concentration,
- (b) the size and dispersion of the particles,
- (c) the level of interfacial adhesion,
- (d) the inherent ductility of the matrix,
- (e) the shear modulus and glass transition temperature (T_g) of the rubber,
- (f) the craze initiation stress and shear yield stress of the matrix.

The various theories thus proposed for explanations of rubber toughening may be categorized as follows¹³:

- (1) Energy absorption by the rubber particles.
- (2) Energy absorption by the yielding of the continuous phase; ductility enhanced by strain induced dilation near the rubber occlusion.
- (3) Craze formation involving cavitation and polymer deformation with the craze.
- (4) Shear yielding as a source of energy absorption and crack termination.
- (5) Stress distribution and relief.
- (6) Rubber particles acting as craze termination points and obstacles to crack propagation.

The notched Izod-impact strength vs. composition were plotted as shown in Figure 4. It was found that the impact strength of blends reaches a maximum at 10 wt % of PU for various POM/PU blend system.

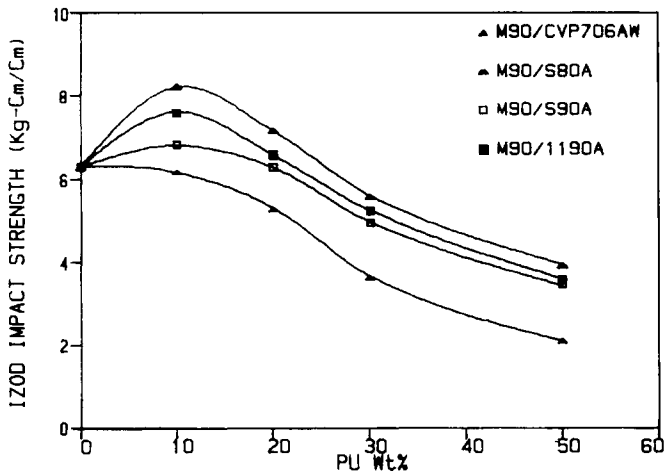


Fig. 4. Izod impact strength of M90/PU blends; (Δ) M90/CVP706AW; (\blacktriangle) M90/S80A; (\square) M90/S90A; (\blacksquare) M90/1190 A.

At the same composition, the effectiveness of POM/PU blends is POM/S80A > POM/1190A > POM/S90A > POM/CVP706AW. While the hardness of PU is shore A 90, the ether-based PU is much more effective in increasing the impact strength of POM/PU blends than that of ester-based PU. While the hardness of PU is larger than shore A 80, the soft PU has much more effectiveness in increasing the impact strength of POM/PU blends than that of hard PU.

X-Ray Diffraction Measurements

The X-ray diffraction scans of polymer blends with weight fraction of PU as a function of the Bragg angle are shown in Figure 5. It shows that, as the content of PU increases, the crystalline diffraction peak becomes weaker. However, the position of the peak is independent of the composition, as expected. It is obvious that the unit cell dimensions of POM remain unchanged.¹⁴ This result is the same as for the POM/EPDM⁶ blend.

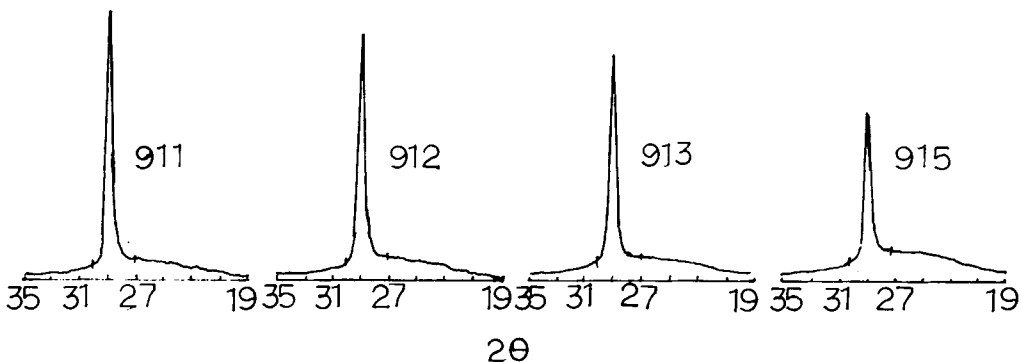


Fig. 5. Intensity distribution of M90/1190A blends.

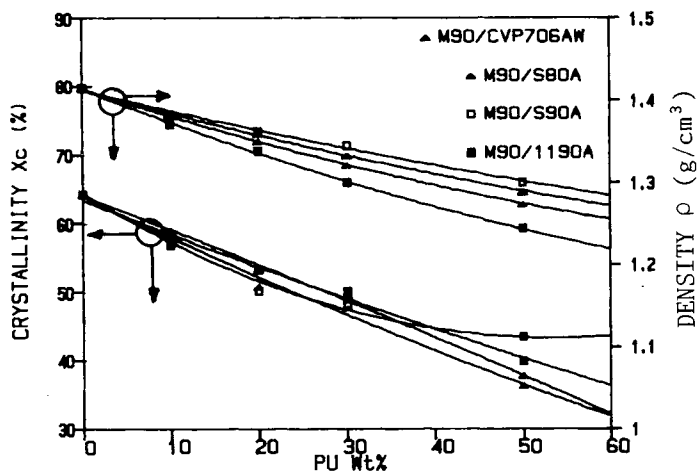


Fig. 6. X_c and density of M90/PU blends: (Δ) M90/CVP706AW; (\blacktriangle) M90/S80A; (\square) M90/S90A; (\blacksquare) M90/1190A.

The crystallinity and the density of the blends decrease with increasing amounts of PU. The result was shown in Figure 6.

Thermogravimetry Analysis

A DuPont 1090B analyzer equipped with a 951-TGA was employed for thermal decomposition detection using a heating rate $20^\circ\text{C}/\text{min}$. The TGA analysis of POM/PU blends was shown in Table II. This table shows that the thermal stability ranking in all systems is

10 wt % PU > 20 wt % PU > 30 wt % PU > 50 wt % PU > pure material

Dielectric Properties

When a polar polymer is placed in an electric field, the polar group in the polymer will tend to orient in that field. If the polymer is very flexible, or at least if the polymer groups are flexible, they will orient easily and quickly. Thus, in an alternating electric field, the polar groups in a polymer will orient and give high dielectric constant values. For this reason, the dielectric constant of blends increases with increasing PU content. This result is the same as that of rubber/epoxy blends.¹⁵ The results are shown in Figure 7.

The dissipation factor is the ratio of conductance to susceptibility of a plastic dielectric and is a measure of the conversion of reactive power to real power, showing up as heat.¹⁶ The modulus and dissipation factor are functions of mobility. The crystallinity of the blends decreases with increasing amounts of PU. A higher crystallinity should result in a lower dissipation factor. In Figure 8, the dissipation factor of the blends increases with increasing concentration of PU.

Volume resistivity is the extent to which a current can pass through the bulk of plastics, and is dependent on the nature of the plastic itself.¹⁶ From the above description, it is known that the volume resistivity decreases with increasing PU content. This result is shown in Figure 9.

TABLE II
TGA Decomposition Temperature of M90/PU Blends

Sample	T_1^a	T_{50}^b	$R_{700}(\%)^c$
CVP706AW	284.5	399.0	2.472
S80A	287.6	393.8	6.425
S90A	290.9	384.5	7.232
1190A	305.9	395.5	4.988
M90-02	325.2	382.8	0.000
971	310.1	422.2	0.961
972	309.2	408.3	1.248
973	308.4	406.9	2.831
975	307.1	400.4	2.163
981	311.9	414.4	0.287
982	311.1	410.5	1.088
983	304.0	399.8	1.645
985	296.9	395.2	5.248
991	325.3	425.5	0.261
992	314.3	415.3	2.693
993	309.2	411.4	5.721
995	306.2	404.0	7.610
911	317.9	430.2	0.206
912	310.9	427.2	0.236
913	306.2	419.2	0.394
915	303.8	420.5	3.988

^a T_1 = 1% weight loss temperature.

^b T_{50} = 50% weight loss temperature.

^c R_{700} = residual weight percent at 700°C.

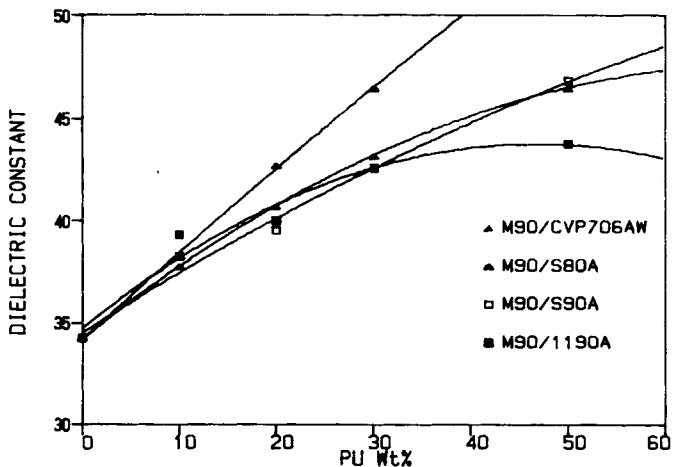


Fig. 7. Dielectric constant of M90/PU blends: (Δ) M90/CVP706AW; (▲) M90/S80A; (□) M90/S90A; (■) M90/1190A.

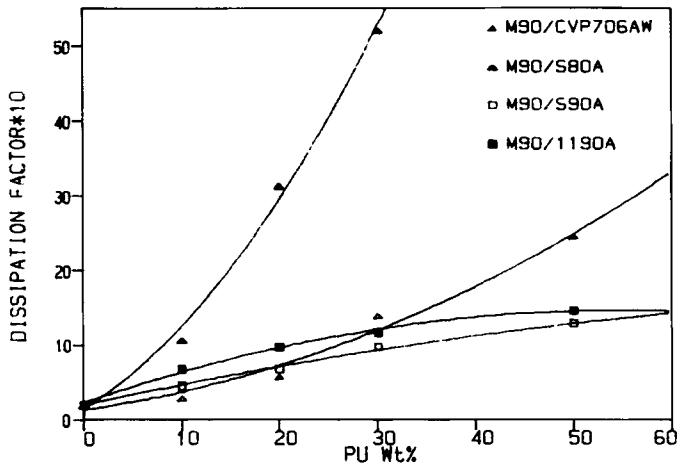


Fig. 8. Dissipation factor of M90/PU blends: (Δ) M90/CVP706AW; (\blacktriangle) M90/S80A; (\square) M90/S90A; (\blacksquare) M90/1190A.

Dynamic Mechanical Measurement

The dynamic mechanical behavior of polymers is of great interest. Damping is often the most sensitive indicator of all kinds of molecular motions which are going on in a material, even in a solid state.¹⁷ Figures 10–12 illustrated the dynamic mechanical properties curve of POM/PU blends as a function of temperature. At the point where the modulus–temperature curve has an inflection point, the damping curve goes through a large maximum. The damping in these curve is expressed as the ratio of the loss modulus or imaginary modulus E'' to the real part of the modulus E' or its equivalent, $\tan \delta$. The imaginary modulus is a term proportional to the energy dissipated as heat, which goes through a less prominent peak than $\tan \delta$, and the

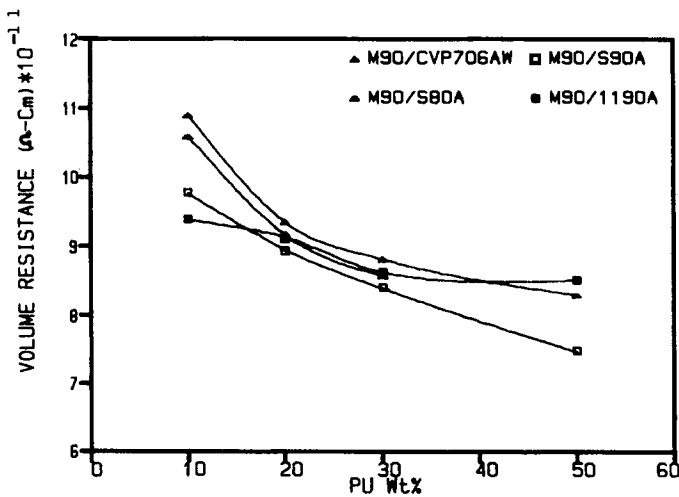


Fig. 9. Volume resistivity of M90/PU blends: (Δ) M90/CVP706AW; (\blacktriangle) M90/S80A; (\square) M90/S90A; (\blacksquare) M90/1190A.

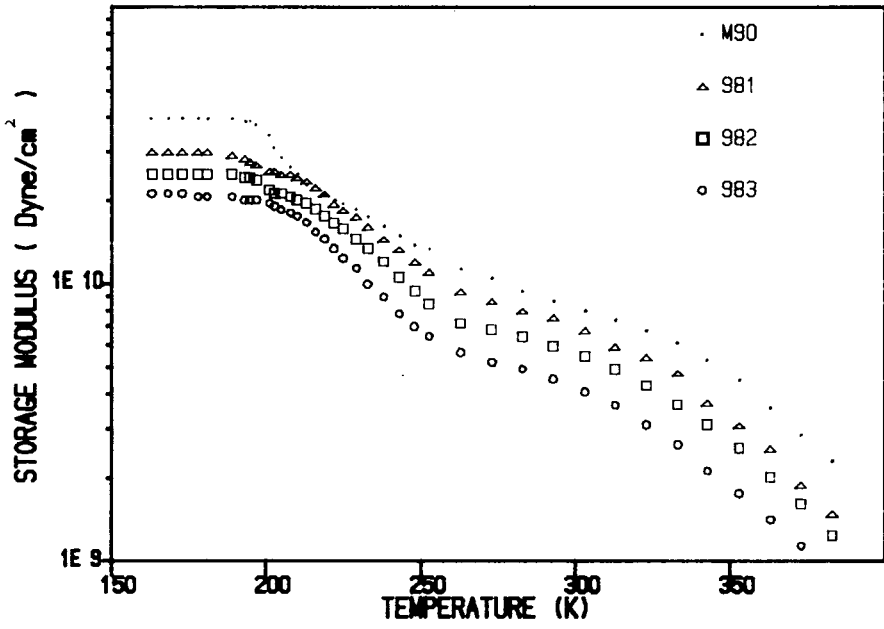


Fig. 10. Storage modulus of M90/S80A blends: (·) M90; (Δ) 981; (□) 982; (○) 983.

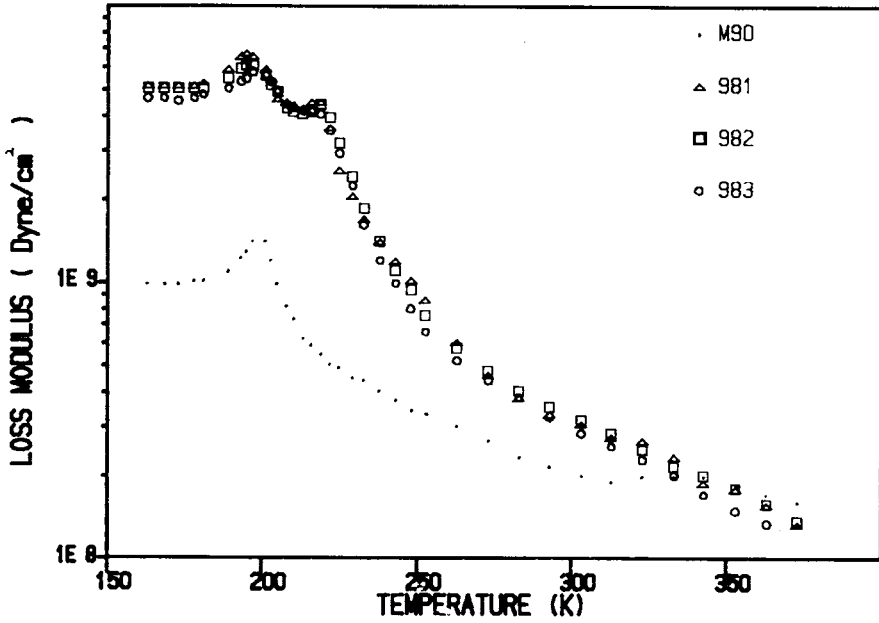


Fig. 11. Loss modulus of M90/S80A blends: (·) M90; (Δ) 981; (□) 982; (○) 983.

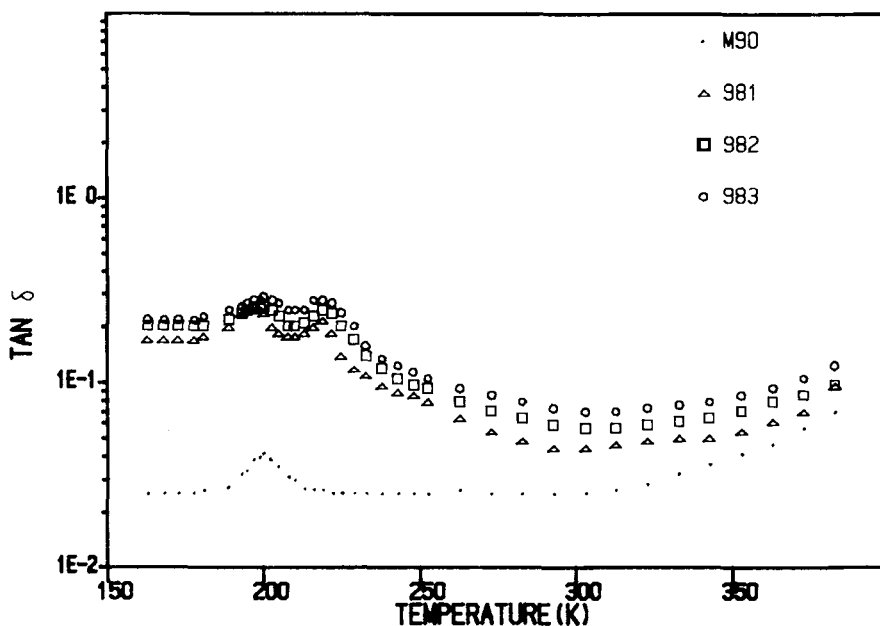


Fig. 12. Loss tan of M90/S80A blends: (·) M90; (Δ) 981; (\square) 982; (\circ) 983.

maximum in the E'' curve occurs at a slightly lower temperature than the peak in the E''/E' or $\tan \delta$ curve. The damping peak is associated with the partial loosening of the polymer structure so that groups and small chain segments can move. The data in Figure 12 show a prominent relaxation peak for POM at -73°C , and this was labeled γ_1 by Hojfors et al.¹⁸ The T_g of POM are -73 and -64°C , at 11 and 110 Hz, respectively. The T_g and maximum in the damping peak are increased by about 9°C as a result of a 10-times increase in frequency. Figure 12 shows that, as PU content increases, only the height of the damping peak will change, but there is no transition temperature shift. This result is similar to that of POM/EPDM⁶ blends but different from that of PC/ABS¹⁹ blends. This indicates that the miscibility of POM and PU is poor. From Figure 10, it was found that the E' decreases with increasing PU content. Figure 12 shows that the $\tan \delta$ of blends increase with increasing PU content.

Figures 13–15 show the dynamic mechanical measurement of POM/PU(90/10) blends. From the damping peak vs. temperature curve (Fig. 15), it was found that the best adhesion of POM/PU blends is the POM/1190A system because it reflects a small damping height. For POM/ester-based PU blends, the soft PU has higher damping peak values than that of hard PU.

Glass Transition

The glass transition temperature T_g of POM is a long-standing problem. The T_g values, reported in the literature,^{18,20–26} range from 50 to 400 K. Variations in five mechanical relaxations in POM copolymers in the temperature range from 4 to 400 K are described as a function of comonomer size and amount. The δ relaxation is interpreted as being due to limited motions in

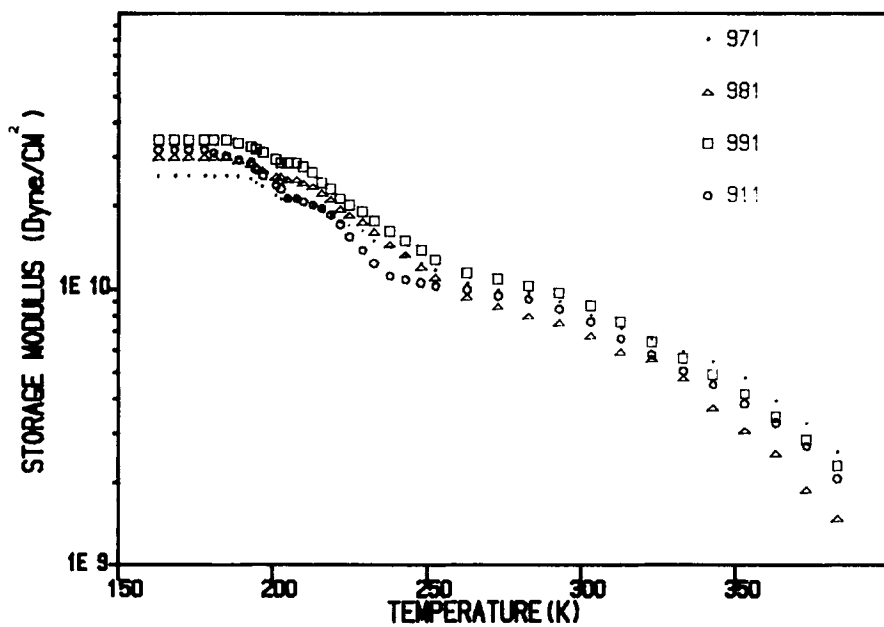


Fig. 13. Storage modulus of M90/PU (90/10) blends: (·) 971; (Δ) 981; (\square) 991; (\circ) 911.

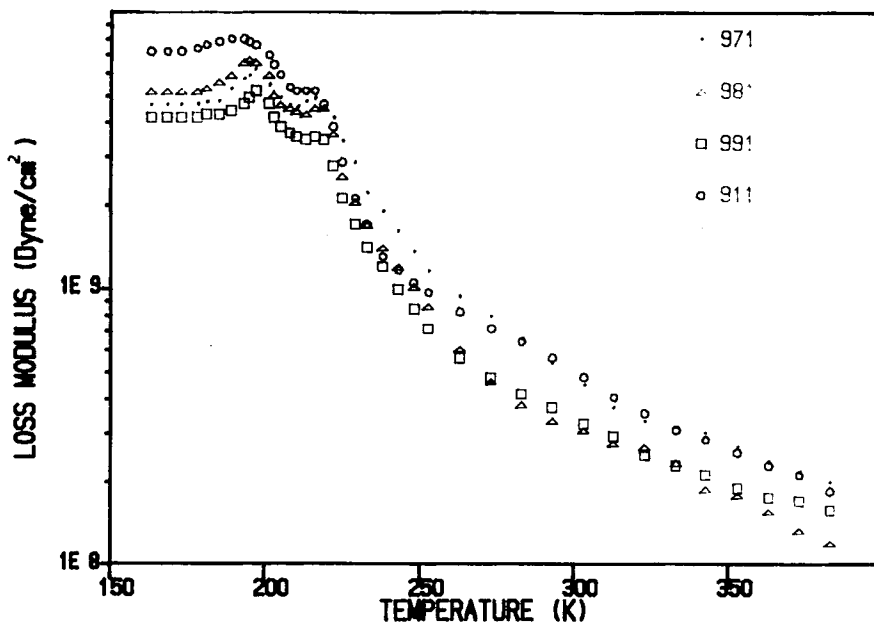


Fig. 14. Loss modulus of M90/PU (90/10) blends: (·) 971; (Δ) 981; (\square) 991; (\circ) 911.

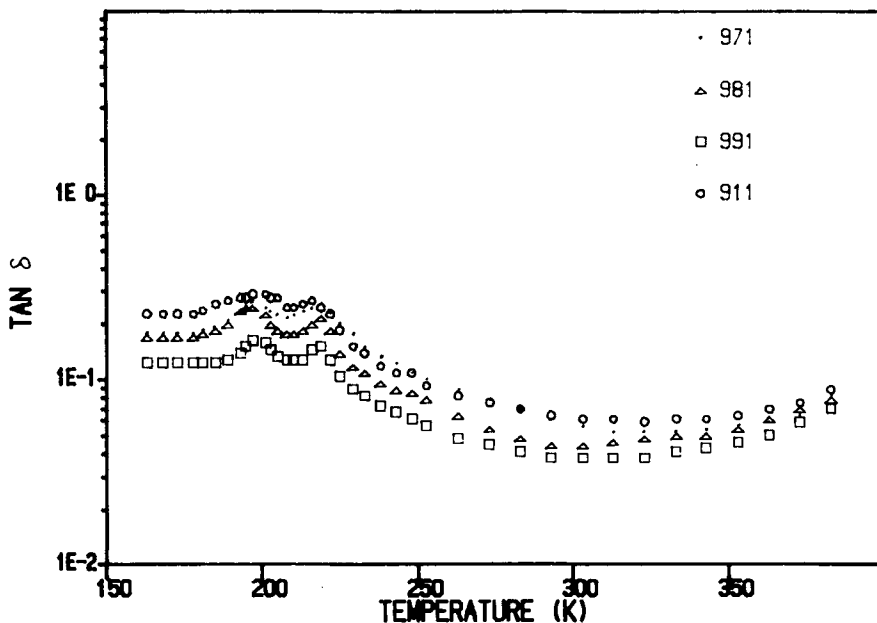


Fig. 15. Loss tan of M90/PU (90/10) blends: (·) 971; (Δ) 981; (\square) 991; (\circ) 911.

defect crystals. The γ_2 relaxation [$T < T_g(L)$] is also associated with defect motion in the crystal and the γ_1 relaxation [$T_g(L)$] is suggested to involve motion of short segments in disordered regions. The β relaxation [$T_g(U)$] involves motion of long segments and the α relaxation (T_{ac}) is generally believed to be associated with the crystalline phase, involving translational motions along the chain axis.¹⁸ Table III indicates the transition observed by a variety of methods.

The existence of a general relationship between amorphous-phase glass-transition temperature T_g and the crystalline-phase melting-transition temperature T_m has long been recognized and most commonly expressed as the two-thirds rule.¹⁷

TABLE III
Transition Temperature (K) for POM^a

Ref. No.	Method	δ	γ_2	γ_1	β	α	T_m
6 ^b	DM	—	—	209	—	375	434.6
This work ^c	DM	—	—	200	—	—	434.6
20	DT	—	—	—	295–358	375	—
18	TP	50	175	205	270	—	—
21	ESR	—	—	—	257	—	—
23	DM	—	—	213	—	—	—
24	RR-HD	—	—	198.2	—	—	—
25	DM	—	188	253	313–323	408	—

^aDM = dynamic mechanical; DT = dilatometry; TP = torsion pendulum; RR-HD = relative rebound-height data; ESR = electron spin resonance.

^bTest frequency 110 Hz.

^cTest frequency 11 Hz.

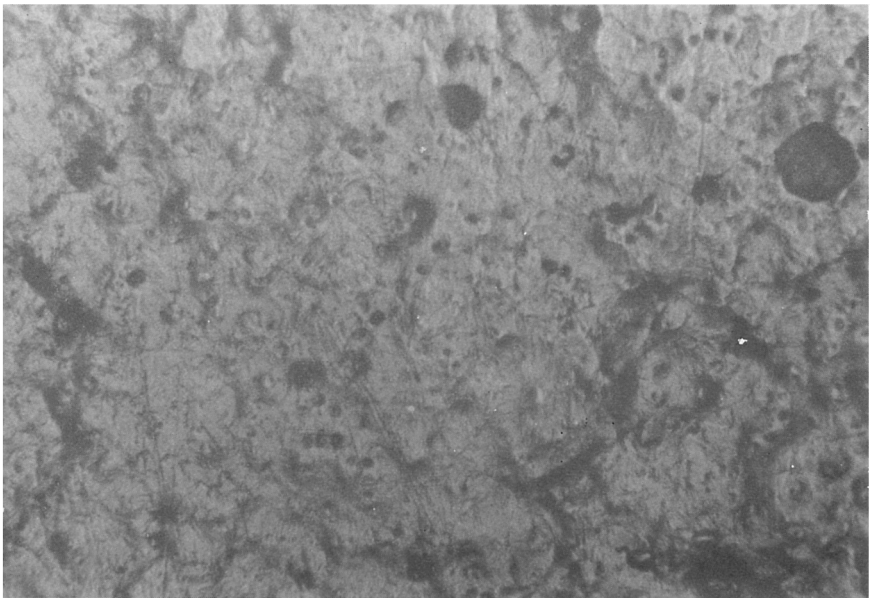
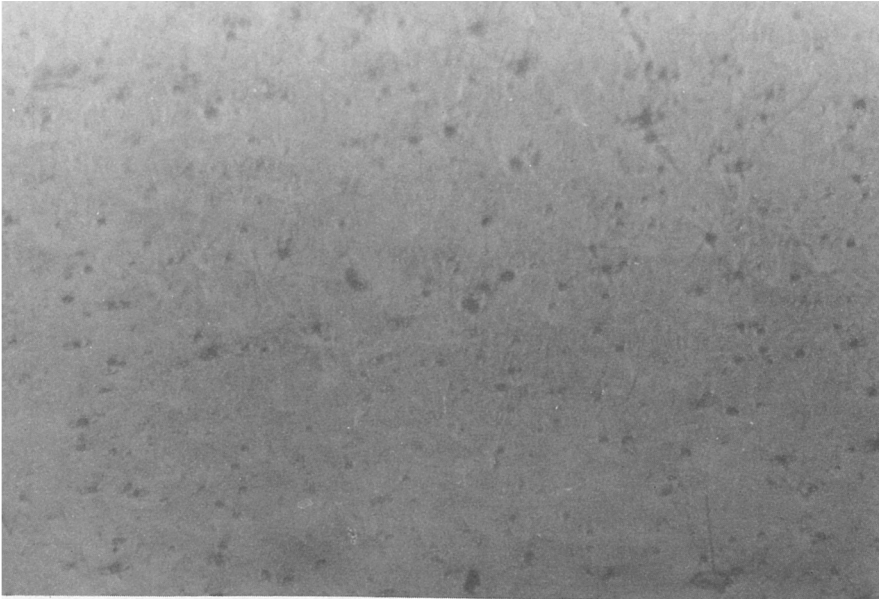


Fig. 16. Metallurgical micrographs of M90/1190A blends.

Boyer²⁵ previously studied the unsubstituted polymers. Unsubstituted polymers can be represented by $[(CH_2)_nR]_p$, where R is CH_2 , CF_2 , O, S, or $CH=CH$; and where n can vary from 0 to ∞ . It was found that the ratio $T_g(L)/T_m$ is not a constant, but is close to 0.5. Enns and Simha²⁰ mention that the ratio $T_g(L)/T_m = 0.47$ is characteristic of symmetrical polymers. The result of this work coincides with that of Enns' description.

Morphology

Compression-molded plastic of the blends was examined under the metal-lurgical microscope to determine phase morphology. Figure 16 shows a comparison of spherulites crystallized from melts of various compositions. These results indicate that the crystalline materials in the pure POM and the blends exist in spherulitic structure. This spherulitic structure has been reported

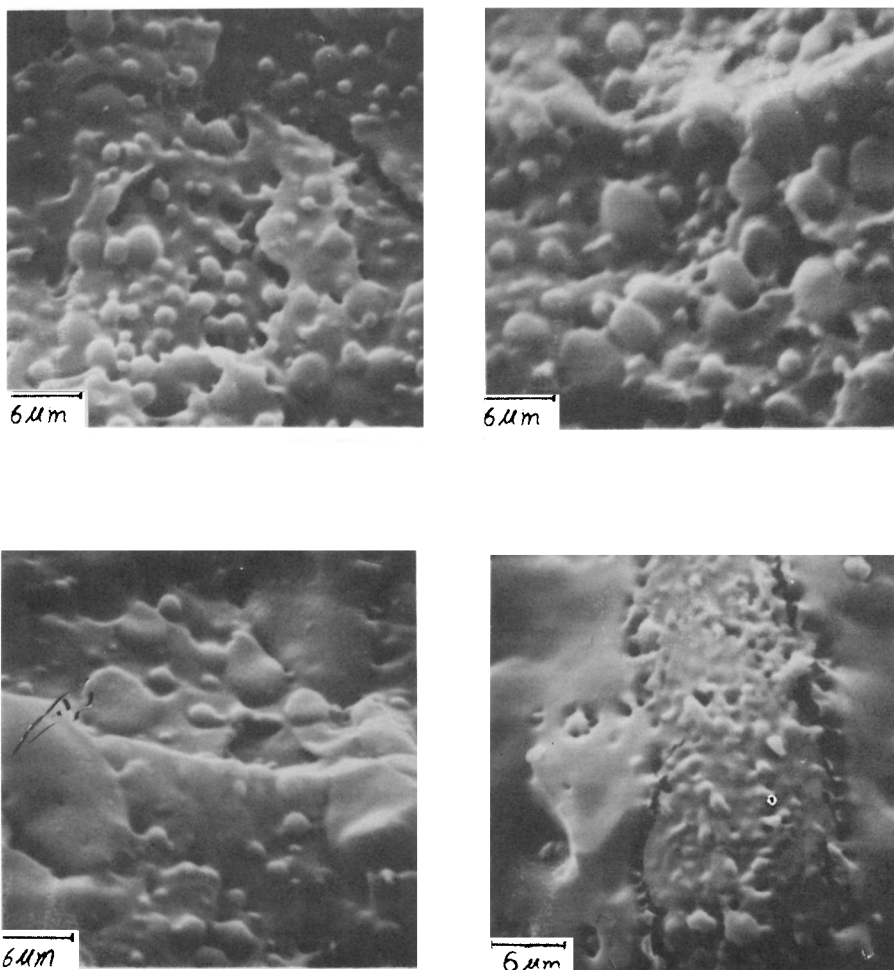


Fig. 17. SEM micrographs of M90/S80A blends.

previously.^{1,5,27,28} From Figure 16, it was found that the spherulitic morphology became ambiguous with increasing concentrations of PU. The presence of elastomer interferes with the growth of spherulites of POM. This result is the same as that of POM/EPDM⁶ blends which were examined by polarized microscope.

SEM micrographs of the cryofractured surfaces of the samples are shown in Figures 17 and 18, from which the morphology can be more clearly seen. The POM/PU 90/10, 80/20, and 70/30 blends show PU islands in a POM sea. The cross section of the discrete islands have dimensions of 1–10 μm depending on composition. From Figures 17 and 18, it was found that the spherical sizes of the dispersed PU, either ether-based PU or ester-based PU, are in the neighborhood of 1–3 μm in diameter at the composition of 10 wt % PU. When containing the composition of 20 wt % PU, the blends exhibit larger spherical domains of PU from 3 to 5 μm . Besides the two-phase state observed in the

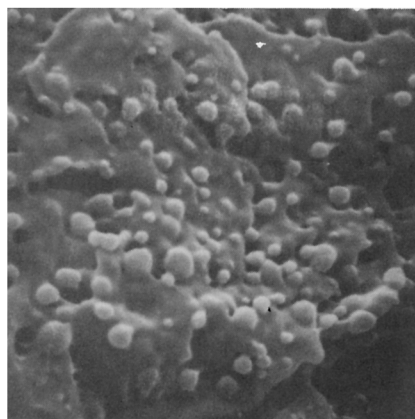
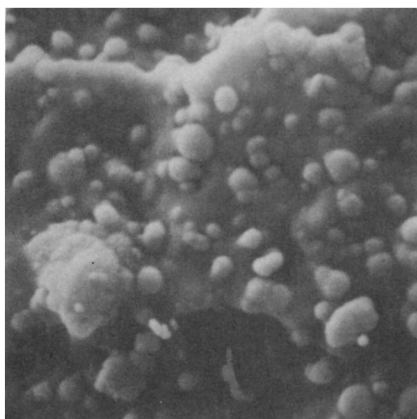
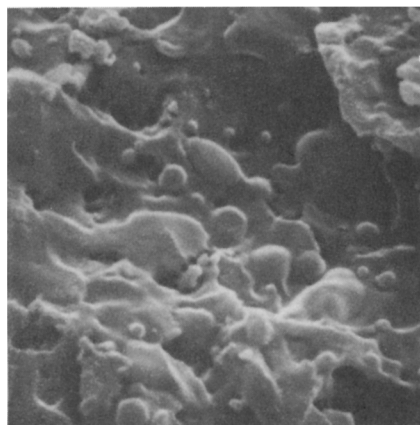


Fig. 18. SEM micrographs of M90/PU (90/10) blends.

other POM/PU blends, it was found that the size of PU particles increased with an increase of PU content in the blend, and that PU and POM both existed in a continuous phase, i.e., phase inversion occurred at a 50/50 composition. This result differed from that of POM/EPDM⁶ blends. The PU particles are spherical in shape with spherical inclusions of the POM matrix, since spherical particles of dispersed PU have the lowest energy in most compositions.²⁹

The domain size at inversion point ($N_c \rightarrow 1$) will be taken to be 150 \AA .³⁰ N_c is the compatibility number.

When $N_c \rightarrow \infty$, compatible system

When $N_c \rightarrow 1$, semicompatible system

When $N_c \rightarrow 0$, incompatible system

Kaplan³⁰ suggested that the 150 \AA was a "universal" constant. Such findings indicate that a domain size of 0.015 \mu m for $N_c = 1$ is not a universal constant as had been proposed,³¹ but is strongly dependent upon the nature of the polymers involved in the blends.

The domain size of PU of 10 wt % PU blends varied from 1 to 3 \mu m . According to Kaplan's reports, the N_c values of this investigation vary from 0.015 to 0.005. The POM/PU system of this work is referred to as an incompatible system. In conclusion, the relation between miscibility characteristics and domain size is a complex one, dependent not only upon the degree of miscibility, but evidently also on the nature of blend components and the test method.

CONCLUSION

The properties of blends are evidence of various degrees of mutual influence between the two components of a blend. The important factor deciding whether properties are enhanced through blending is the miscibility and interaction between the two components. A well-compatible blend might have a profound effect on toughness improvement without noticeably sacrificing the strength to any significant extent.

The notched Izod-impact strength of blends reached a maximum at 10 wt % PU. The tensile strength decreased by second-order with PU content and the Young's moduli decreased with increasing concentration of PU.

The degree of crystallinity and the density of the polymer blends decreased with increasing content of PU. For POM/PU blends, the thermal stability tendency of all systems is

10 wt % PU > 20 wt % PU > 30 wt % PU > 50 wt % PU > pure materials

From dynamic mechanical measurements, the POM/PU systems are incompatible. In this work, T_g/T_m clusters around a value of about $2/3$ but has an extreme range of POM about 0.460. The N_c values vary from 0.015 to 0.06. This shows that the POM/PU systems are incompatible.

The authors wish to express their sincere appreciation to Dr. T. S. Lin, President of Tatung Institute of Technology, for his encouragement and support.

References

1. R. W. Hertzberg, M. D. Skibo, and J. A. Manson, *J. Mat. Sci.*, **13**, 1038 (1978).
2. C. B. Bucknall, *Toughened Plastics*, Applied Science, London, 1977.
3. S. Y. Hobbs, R. C. Bopp, and V. H. Watkins, *Polym. Eng. Sci.*, **23**, 380 (1983).
4. E. A. Flexman, Jr., *Mod. Plast.*, **62**, 72, 74, 76 (1985).
5. W. Y. Chiang and M. S. Lo, *J. Appl. Polym. Sci.*, **36**, 1685 (1988).
6. W. Y. Chiang and C. Y. Huang, *Polym. Eng. Sci.*, to appear.
7. K. Matsuzaki, Jpn. Pat. 60,104,116 (1985); *Chem. Abstr.*, **103**, 179108m (1985).
8. K. Matsuzaki and M. Hamada, Jpn. Pat. 60,144,352 (1985); *Chem. Abstr.*, **103**, 216319d (1985).
9. K. Matsuzaki and M. Hamada, Jpn. Pat. 60,144,353 (1985); *Chem. Abstr.*, **103**, 196927v (1985).
10. E. Reske and E. Wolters, Ger. Offen. DE 3,303,760 (1984); *Chem. Abstr.*, **101**, 172445u (1984).
11. D. Yang, B. Zhang, Y. Yang, Z. Fang, G. Sun, and Z. Feng, *Polym. Eng. Sci.*, **24**, 612 (1984).
12. J. A. Manson and L. H. Sperling, Eds., *Polymer Blends and Composites*, Plenum, New York, 1976.
13. D. R. Paul and S. Newman, Eds., *Polymer Blends*, Academic, New York, 1978, Vol. 1.
14. C. J. Ong and F. P. Price, *J. Polym. Sci., Polym. Symp.*, **63**, 45 (1978).
15. C. Domenici, G. Levita, A. Marchetti, and V. Frosini, *J. Appl. Polym. Sci.*, **34**, 2285 (1987).
16. S. S. Schwartz and S. H. Goodman, Eds. *Plastics Material and Processes*, Van Nostrand Reinhold, New York, 1982.
17. L. E. Nielsen, *Mechanical Properties of Polymers and Composites*, Dekker, New York, 1974, Vol. 1.
18. R. T. V. Højfors, E. Baer, and P. H. Geil, *J. Macromol. Sci. Phys.*, **B13**, 323 (1977).
19. W. Y. Chiang and D. S. Hwang, *Polym. Eng. Sci.*, **27**, 632 (1987).
20. J. B. Enns and R. Simha, *J. Macromol. Sci. Phys.*, **B13**, 25 (1977).
21. P. L. Kumler and R. F. Boyer, *Macromolecules*, **9**, 903 (1976).
22. V. P. Privalko, *Polym. Sci. U.S.S.R.*, **18**, 1392 (1976).
23. B. Brew, J. Clements, G. R. Davies, R. Jakeways, and I. M. Ward, *J. Polym. Sci., Polym. Phys. Ed.*, **17**, 351 (1979).
24. A. A. Blumberg and E. R. Niemira, *J. Polym. Sci., Polym. Phys. Ed.*, **17**, 1891 (1979).
25. R. F. Boyer, *Br. Polym. J.*, **14**, 163 (1982).
26. H. Suzuki, J. Grebowicz, and B. Wunderlich, *Br. Polym. J.*, **17**, 1 (1985).
27. Z. Pelzbauer and A. Galeski, *J. Polym. Sci.*, **C38**, 23 (1972).
28. W. Y. Chiang and M. S. Lo, *J. Appl. Polym. Sci.*, **34**, 1997 (1987).
29. S. Bywater, *Polym. Eng. Sci.*, **24**, 104 (1984).
30. D. S. Kaplan, *J. Appl. Polym. Sci.*, **20**, 2615 (1976).
31. O. Olabisi, L. M. Robeson, and M. T. Shaw, *Polymer-Polymer Miscibility*, Academic, New York, 1979.

Received July 21, 1988

Accepted October 26, 1988